

Energy flux of electron precipitation as monitored by an all-sky camera

K. Kauristie, N. Partamies, S. Mäkinen, R. Kuula, and A. Strømme

Abstract: We use the inversion method of [4] to estimate the energy flux of electron precipitation from the emission rates recorded by our All-Sky Camera in Kilpisjärvi (KIL). The beam of the incoherent scatter radar EISCAT is in the central field of view of the camera which enables comparisons of the ASC and radar based precipitation flux estimates. Our data set of 533 pairs of simultaneous flux estimates show a correlation of $r = 0.72$ between the two data sets. In global scale the energy flux of auroral precipitation is known to have a linear correlation with the AE-index. We find a similar relationship between the energy flux as integrated over the KIL ASC field-of-view and the local auroral electrojet index defined from the IMAGE magnetometer chain (IE-index). The linear relationship holds especially when the epsilon parameter of solar wind input stays below 0.2 TW (as 10 min averages) and then one can see 10-20% of the global auroral precipitation energy flux with one ASC located in the midnight sector.

Key words: auroral precipitation, all-sky cameras, substorms.

1. Introduction

The inversion method by [4] (hereafter ASCinv) can be used to estimate the energy flux of electron precipitation from the basis of multiwavelength All-Sky Camera (ASC) observations. The method makes the inversion from ASC data to volume emission rates and to the corresponding energy flux as a single step. The energy range of the method is 0.1–8 keV. The coupling between the energy deposition of the electron precipitation and the auroral emission is modelled with the empirical formulas of [9, 10] and [11]. [8] evaluate the performance of ASCinv by comparing its output with flux estimates as deduced from DMSP and EISCAT data. The study demonstrates that in favourable conditions (stable arc near the ASC zenith) ASCinv estimates of electron energy flux agree within 10% relative error with the DMSP flux measurements. Using the modifications suggested by [12] in the emission physics yields better consistency between the two data sets. With EISCAT based flux estimates (deduced with the SPECTRUM method of [6]) the correlation is less obvious: smaller than 50% relative errors were found only in 36% of the analysed cases. The differences between the energy range and time resolution of ASCinv and SPECTRUM at least partly explain the inconsistencies in the flux estimates. The analysis of [8] also revealed that ASCinv reproduces more reliably the energy flux values than the number flux values.

In this paper we continue the comparison study of EISCAT and ASC based electron flux estimates. While [8] selected for their analysis individual images with stable auroras in the EISCAT beam location, we use here events of longer duration (and thus not always auroras in the EISCAT measurement point) to search some general trends in the flux estimate inconsistencies.

Probing the performance of ASCinv in different conditions is an intermediate step to reach our final goal which is the routine usage of ASC-data for monitoring mesoscale energy dissipation due to auroral precipitation similarly as local AE-indices are used to monitor Joule heating rates. The latter part of this paper we study mesoscale energy dissipation with ASC-recordings during 17 substorm periods and discuss the relation between local and global energy consumption rates.

2. ASC-EISCAT comparisons

The events for the EISCAT-ASC comparison study were selected carefully in order to avoid periods with clouds or too bright auroras which saturate the camera. Auroral brightnesses around 2-7 kR appeared to be suitable for our analysis. The point in the ASC image comparable with the EISCAT observation depends naturally on the altitude of the auroras. The altitude could be estimated for each time separately e.g. by investigating the EISCAT electron density profiles. In this study, however, we used the constant beam location of 69.4 N and 19.2 E, which corresponds to the altitude of 110 km. Using a constant location for all the events may cause additional scatter especially in the cases where the assumed altitude is slightly erroneous and there are sharp gradients in the precipitation around the EISCAT beam location. In these cases EISCAT measurements may come from a dark region while ASC recordings come from bright region (or vice versa).

The electron precipitation which typically causes 557.7 nm auroras has average energies around 2–20 keV and thus it increases electron densities at altitudes 95–130 km [10]. In Fig. 1 we test how accurately the KIL ASC and EISCAT observations follow this principle. The data have been recorded during five 1–2 hour long periods of moderate substorm activity. The plotted parameters are the ASCinv energy flux from KIL ASC data and the electron content along the EISCAT field line as integrated over 95–130 km altitudes. The electron content show increasing trend with increasing energy fluxes like it should, but the scatter of the data points is large especially at the high flux values. The linear fit between the points is TEC

Received 17 May 2006.

K. Kauristie and S. Mäkinen. Finnish Meteorological Institute, Space Research, P.O.Box 503, FIN-00101 Helsinki, Finland.

N. Partamies. Institute for Space Research, University of Calgary, Alberta, Canada.

R. Kuula. University of Oulu, Finland

A. Strømme. EISCAT Association, Sweden

$\times 10^{-16} = 166.40(\text{Wm})^{-1} \times \text{Eflux} + 1.01 \text{ m}^{-3}$ with $r = 0.66$.

Precipitation causing visual auroras increases especially the ionospheric Hall conductances. Thus in the auroral regions the ratio of Hall to Pedersen conductance (hereafter the α -parameter) is enhanced and in substorm auroras it can vary in the range 1–5 [2]. Fig. 2 shows the dependency of the α -values by EISCAT on the energy flux values by ASCinv. In the flux range from 3–10 mW/m^2 the majority of data points show roughly a linear relationship with the α -values increasing from 0.5 to 2.3. This picture is obscured somewhat by a secondary branch of points which show high α -values for minimal flux values. These α -values, however, are less significant as they have been measured in dark conditions where both Hall and Pedersen conductances have been small (c.f. the group of points with $\text{TECU} < 1$ in Fig. 1).

The relationship between the energy flux estimates by EISCAT computed with the SPECTRUM program [6] and the flux values by ASCinv are shown in Fig. 3. This data set suggests that EISCAT-based flux values tend to be slightly larger than the ASCinv based flux values. The linear fit best describing this relationship is $\text{Eflux}_{\text{EISCAT}} = 1.35 \times \text{Eflux}_{\text{ASCinv}} - 0.70 \text{ mW/m}^2$ with $r = 0.72$. Obviously the data set should be expanded with more events having energy flux values above 15 mW/m^2 to get further confirmation for this result.

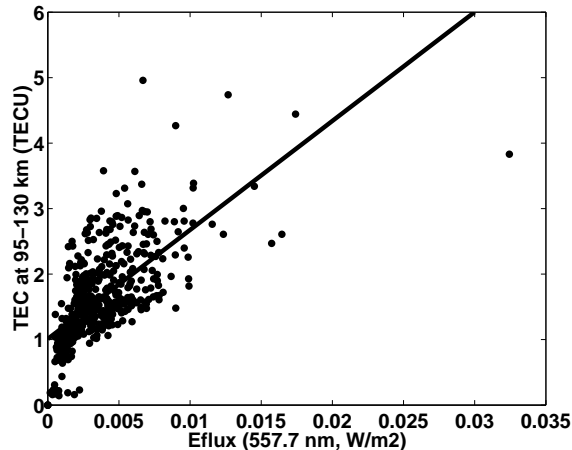


Fig. 1. Energy flux as deduced from ASC data versus the electron content along the EISCAT field line and integrated over 95–130 km altitudes ($\text{TECU} = 10^{16} \text{ m}^{-3}$). The number of data points is 486 and $r = 0.66$ for the linear fit.

3. Precipitation power over ASC field-of-view

In order to study the auroral precipitation power in meso-scales we integrate the energy flux values by ASCinv over the field-of view of the KIL ASC which is a circle of $\sim 300 \text{ km}$ radius. The original size of an ASC image is 512×512 pixels which corresponds to a spatial resolution in the range from about one km (near the zenith) to tens of km (near horizon). We use in the integration 8×8 superpixels, i.e. a grid of 64×64 points and again the situations of intensity saturation are avoided (i.e. we handle only luminosities between 2–7 kR).

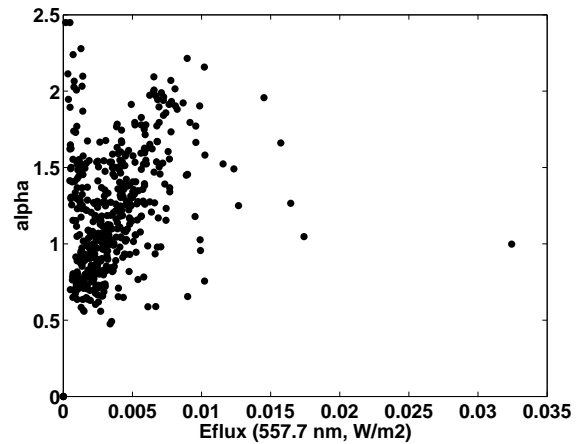


Fig. 2. Energy flux as deduced from ASC data versus the Hall to Pedersen conductance ratio (α). The number of data points is 486.

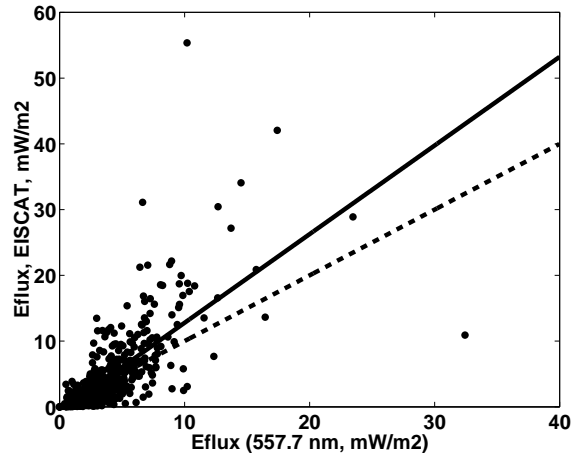


Fig. 3. Energy flux as deduced from ASC data versus the flux values computed from EISCAT data with the SPECTRUM-programme. Dashed line shows the one-to-one correspondence. Solid line shows the best linear fit with $r = 0.72$. The number of data points is 533.

Our data set consists of 17 1–2 hour periods of substorm activity with one minute time resolution which corresponds to 2290 ASC-fov-power values.

3.1. MLT distribution

Fig. 4 shows the distributions of ASC-fov-power values in the different MLT-sectors. In the evening and midnight sectors the distributions have the peak at the values 1–2 GW and the occurrences of the higher power values show an exponential decay. In the morning sector the distribution has in addition to the main peak at 1–2 GW another maximum at 4–6 GW. The morning sector distribution is consistent with the previous findings by [7] of enhanced energy dissipation in the morning sector during substorms.

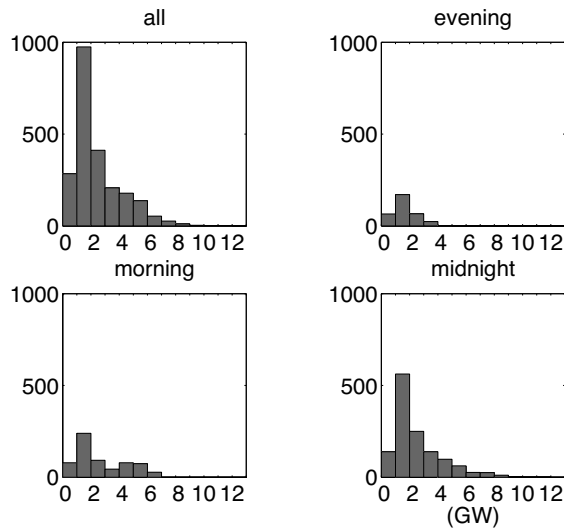


Fig. 4. Distributions of the ASC-fov-power values in the different MLT sectors: Evening sector 17.5–21.5 MLT, morning sector 3.5–8.5 MLT, and midnight sector 21.5–3.5 MLT.

3.2. Connection with the electrojet activity

ASC-fov-power can be anticipated to correlate with electrojet activity only during moderate activity when the oval is at the latitudes of KIL (MLAT ~ 66) and the ASC field-of-view monitors a significant portion of the auroral oval. We characterize the global activity level with the solar wind energy input as estimated with the Akasofu ϵ -parameter [3]. ϵ is computed from the data of the ACE satellite and shifted in time according to the propagation time from the satellite to the nominal magnetopause distance ($10 R_E$). In comparisons with the nightside activity it is also reasonable to smoothen out the rapid time variations from the ϵ -parameter. Instead of pure ϵ -values we use the energy values achieved by the time integration of ϵ over the 10-min period preceding each ASC-fov-power observation.

As a measure of electrojet activity we use the IE-index which is derived with the AE-index method from the recordings of the Fennoscandian IMAGE magnetometer chain. When the IMAGE magnetometer chain monitors the MLT-sectors 00–04 the IE-index can be considered as a representative estimate of the global AE-activity [5]. KIL ASC-fov-power values appeared to have the best correlation with IE-values when the solar wind input energy 10-min values stay below 100 TJ (corresponds roughly to 10-min average of $\epsilon \sim 0.2$ TW). Under this condition we can write $E_{\text{flux}} = 0.0071 \text{ (GW/nT)} \times \text{IE} + 0.6 \text{ GW}$ (with $r = 0.68$, c.f. Fig. 5).

3.3. Example event

Our example event is a substorm which took place on Oct 20–21 2004 during 23:00–02:00 UT. The solar energy input, IE-index, and KIL ASC-fov-power recorded during this substorm are shown in Fig. 6. The ϵ -values varied around 0.3–0.4 TW during the hour preceding the substorm onset which was associated with IMF B_Z northward turning and consequent ϵ drop to zero. After a break of ~ 45 the energy input from the solar wind rose up again and ϵ values increased back to level

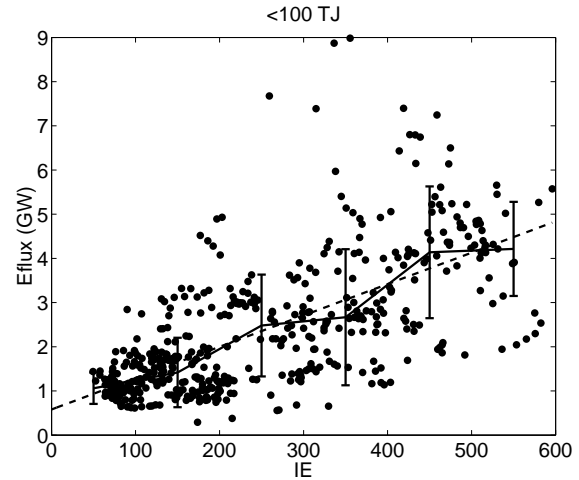


Fig. 5. Dependency between the IE-index and KIL ASC-fov-power when $\int^{10\text{-min}} \epsilon dt < 100$ TJ. Dashed line shows the linear fit with $r = 0.68$. Solid line and the errorbars show the ASC-fov-power median and standard deviation values in bins 0–100 nT, 100–200 nT, 200–300 nT, 300–400 nT, 400–500 nT and 500–600 nT.

0.4–0.5 TW (corresponding to 10-min power values of 100–200 TJ) where it stayed until the recovery of the substorm. According to the AE quicklook plots in the Kyoto WDC website the IE-index represented the global electrojet activity quite well: The duration of the event is roughly the same in both indices and the peak in IE is only ≤ 50 nT smaller than that of AE.

The KIL ASC-fov-power was largest at $\sim 23:50$ UT, i.e. about 15 minutes after the start of onset in the IE-index. The peak value was 5.1 GW while the few values recorded before the breakup were around 0.3 GW and after the expansion phase (i.e. after 00:15 UT) the values remained at the level of 1 GW for 1.5 hours. During the period 23:38–00:15 UT of bright auroras (c.f. Fig. 7 for example images) the energy dissipation in the ionosphere due to electron precipitation was 5.1 TJ and during the recovery phase period 00:15–01:45 UT of dimmer auroras the dissipation was 6.4 TJ.

4. Summary and conclusions

We have investigated the electron precipitation energy flux values as deduced from ASC data with the method of [4]. Our data set of five 1–2 hour periods of substorm activity with simultaneous ASC and EISCAT observations shows a relatively good correlation ($r = 0.72$) between the ASC-based and EISCAT-based energy flux estimates.

We have also studied the variations of the electron precipitation power in the area of one ASC field-of-view (circle with ~ 300 km radius, luminosity range 2–7 kR). In the data set of 17 1–2 hour periods of moderate substorm activity the most typical power values varied between 1–2 GW. Larger values, 5–6 GW, were recorded during the auroral breakups, as can be anticipated, but also during the morning sector auroras.

The ASC-fov-power values of our KIL camera (MLAT ~ 66) correlate with the global electrojet activity if auroras are mon-

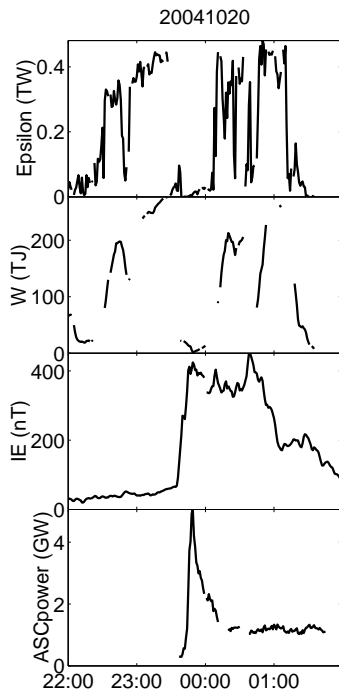


Fig. 6. Energy and power values recorded during the substorm on Oct 20–21 2004. From top to bottom: Solar wind ϵ , energy values achieved by intergating ϵ over the preceding 10 minutes, IE-index from the IMAGE magnetometer chain and KIL ASC-fov-power values.

itored in the MLT-sector 00–04 and if the solar wind input is moderate (10-min ϵ average ≤ 0.2 TW). If we under these conditions use the estimate of [1] for the dependency of global precipitation power on AE-index ($E_{flux}(GW) = 0.06 * AE$ (nT)) together with the corresponding formula for local activity achieved in this study we come to the conclusion that one ASC can see 10–20% of the global precipitation energy in the AE-range of 100–600 nT.

References

1. Ahn, B.-H., Akasofu, S.-I. and Kamide Y., The Joule heat production rate and the particle energy injection rate as a function of the geomagnetic indices AE and AL, *J. Geophys. Res.*, **88**, 6275–6287, 1983.
2. Aikio, A. T. and Kaila, K. U., A substorm observed by EISCAT and other ground-based instruments - evidence for near-Earth initiation, *J. Atmos. Terr. Phys.*, **58**, 5–21, 1996.
3. Akasofu, S.-I., Energy coupling between the solar wind and the magnetosphere, *Space Sci. Rev.*, **28**, 121, 1981.
4. Janhunen, P., Reconstruction of electron precipitation characteristics from a set of multi-wavelength digital all-sky auroral images, *J. Geophys. Res.*, **106**, 18505–18516, 2001.
5. Kauristie, K., Pulkkinen, T. I., Pellinen, R. J. and Opgenoorth, H. J., What can we tell about global auroral-electrojet activity from a single meridional magnetometer chain?, *Ann. Geophys.* **14**, 1177–1185, 1988.
6. Kirkwood, S., SPECTRUM - a computer algorithm to derive the flux-energy spectrum of precipitating particles from EISCAT

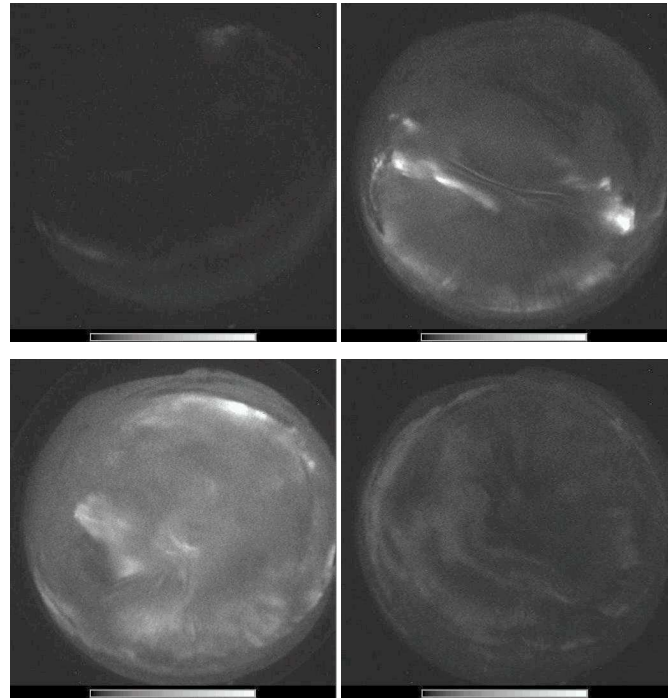


Fig. 7. KIL ASC images (557.7 nm) acquired during the substorm on Oct 20–21 2004. From top left to bottom right: 23:38 UT (growth), 23:45 UT (breakup), 23:48 UT (expansion) and 00:55 UT (recovery).

electron density profiles, *IRF Tech. Rep.*, 034, Swedish Institute of Space Physics, 1988.

7. Opgenoorth, H. J., Persson, M. A. L., Pulkkinen, T. I. and Pellinen, R. J., Recovery phase of magnetospheric substorms and its association with morning sector aurora, *J. Geophys. Res.*, **99**, 4115–4129, 1994.
8. Partamies, N., Janhunen, P., Kauristie, K., Mäkinen, S. and Sergienko, T., Testing an inversion method for estimating electron energy fluxes from all-sky camera images, *Ann. Geophys.*, **22**, 1961–1971, 2004.
9. Rees, M. H., Auroral ionization and excitation by incident energetic electrons, *Planet. Space Sci.*, **11**, 1209–1218, 1963.
10. Rees, M. H., *Physics and Chemistry of the Upper Atmosphere*, Cambridge University Press, New York, 1989.
11. Rees, M. H. and Luckey, D., Auroral electron energy derived from ratio of spectroscopic emissions, 1. Model computations, *J. Geophys. Res.*, **79**, 5181–5186, 1974.
12. Sergienko, T. and Ivanov, V. E., A new approach to calculate the excitation of atmospheric gases by auroral electron impact, *Ann. Geophys.*, **11**, 717–727, 1993.